Powder Technology 285 (2015) 123–127

Contents lists available at ScienceDirect

Powder Technology

journal homepage: www.elsevier.com/locate/powtec

Analysis of the dynamics of the FT4 powder rheometer

C. Hare [a,*], U. Zafar [a], M. Ghadiri [a], T. Freeman [b], J. Clayton [b], M.J. Murtagh [a]

[a] Institute of Particle Science and Engineering, University of Leeds, Leeds LS2 9JT, UK
[b] Freeman Technology, Tewkesbury GL20 8DN, UK

ARTICLE INFO

Available online 24 April 2015

Keywords:
Flowability
Dynamic flow
Powder rheology
DEM
Shear stress

ABSTRACT

Traditional powder flow measurement devices, such as shear cells, operate in the quasi-static regime of shear strain rate. The FT4 powder rheometer of Freeman Technology, developed over the last two decades, has provided a clearer differentiation of powder flowability in some instances. This has been attributed to the instrument operating in the dynamic regime of shear strain rates, a feature that has yet to be established. We report an analysis of the dynamic behaviour of a bed of glass beads made cohesive by silanisation and subjected to standard FT4 testing procedure, where a rotating blade is driven into a cylindrical bed, using a combination of experimental measurements and numerical simulations by the Distinct Element Method (DEM). The DEM analysis underestimates the flow energy measured experimentally, although the agreement is improved when sliding friction is increased. The shear stress of the powder in front of the blade is shown to be roughly constant along the radial direction and increasing as the impeller penetrates the bed, suggesting that a characteristic shear stress can be determined for a powder under a given test condition in the FT4. For ease of simulations large beads were used (1.7–2.1 mm). Future work will investigate the influence of particle properties and operational conditions on the prevailing stresses and strain rates.

1. Introduction

Reliable flow of cohesive powders is very difficult to achieve in many particle process operations, such as discharge from hoppers and bins, feeding, and dosing. Suitable designs of hoppers have long been established by shear cell testing [1], where the shear resistance is characterised at a given consolidation stress or state of packing. This technique is typically carried out at moderate to high stresses and very low shear deformation rates. However there are two aspects of powder flow characterisation that are relevant to powder feeding and dosing that are highly challenging (i) low stresses, and (ii) high strain rates. Recently shear cells have been developed that can provide normal stresses lower than 1 kPa [2], alongside this a number of alternative low stress test methods have been developed, including the Sevilla Powder Tester [3], the Raining Bed Method [4], the SSSPIN Tester [5] and the Ball Indentation Method [6]. These techniques all operate in the quasi-static regime, and the measurement of flowability under higher strain rates has received less attention in the literature. There are many cases where understanding dynamic flow behaviour is critical for process design and operation, e.g. in screw conveyors and mixers. Tardos et al. [7] developed a Couette flow cell consisting of two concentric cylinders with differential rotational speeds, between which the powder was sheared. They characterised the dependency of the shear stress on the strain rate for a number of materials in the quasi-static, intermediate and dynamic regimes, where they showed that the shear stress increased with strain rate in the intermediate and dynamic regimes. The device requires a large quantity of powder and gripping of particles is problematic, which results in descent of powder near the walls [8], consequently refinement is needed to establish this as a suitable dynamic flow characterisation instrument. Pasha et al. [9] simulated the ball indentation technique in the dynamic regime and showed qualitatively similar trends to those of Tardos et al. [7]. This technique is promising, with the added advantage of being applicable with very small quantities of powder, though further investigation into its behaviour in the dynamic regime is required.

In the last ten years the Freeman FT4 Powder Rheometer has emerged as a novel powder flow testing device. The flow resistance is characterised by the flow energy; the summation of the rotational and translational work required to drive a rotating impeller a certain distance into a powder bed. It has been shown to be able to differentiate the flowability of powders that otherwise exhibit similar behaviour under shear testing [10]. This may be attributed in part to the dynamic nature of the test. In other cases the flow energy has correlated well with other flowability measurement techniques [11]. However, the strain rate of the test has not been characterised, and furthermore the stress distribution within the bed has not been determined, although it is claimed that the blade design ensures a constant stress across the width of the impeller. Consequently the device can currently be used only for comparative testing, rather than process design. Bharadwaj

* Corresponding author. Tel.: +44 113 343 2407; fax: +44 113 343 2384.
E-mail address: c.l.hare@leeds.ac.uk (C. Hare).

http://dx.doi.org/10.1016/j.powtec.2015.04.039

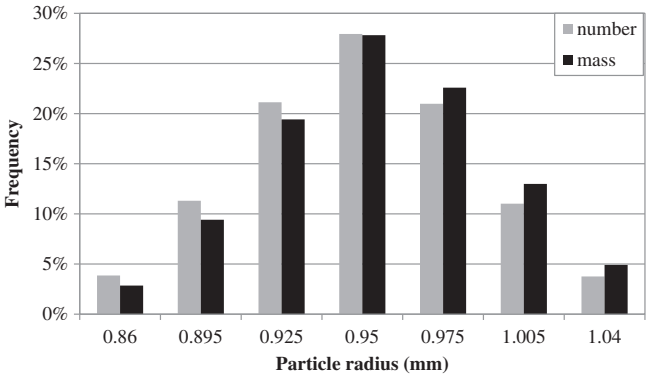

Fig. 1. Size distribution of the simulated glass beads.

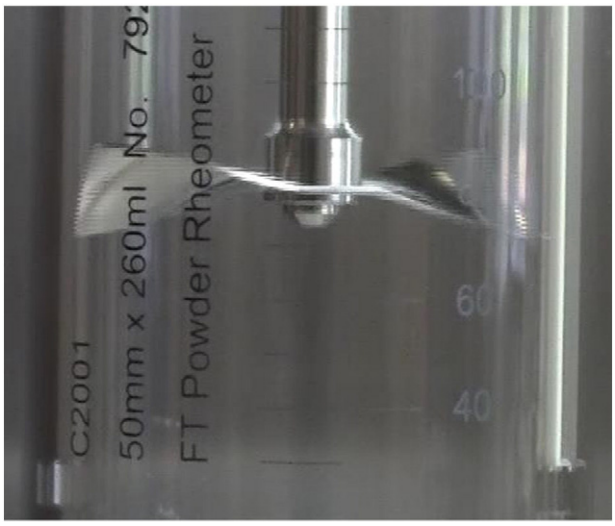

Fig. 2. The 50 mm FT4.

et al. [12] used the Distinct Element Method (DEM) to determine the effects of particle size, shape, size distribution and friction on the force and torque on the impeller in the FT4 Powder Rheometer for a non-cohesive system. Hare et al. [13] characterised the stress and strain rate distribution within an agitated powder bed by the DEM. In this paper we follow a similar approach to analyse the dynamic powder behaviour in the FT4 Powder Rheometer for cohesive particles.

2. Materials and methods

In order to allow for accurate simulations by DEM, 1.7–2.1 mm spherical glass beads are used in this work, with the size distribution given in Fig. 1. These beads are silanised with sigmacote® (with hexane functional group) to provide a cohesive coating layer, whilst size and shape are maintained. In the coating process 250 g of glass beads is mixed with 60 ml of sigmacote® and left on a filet for 30 min, after which vacuum is applied. This process is repeated three times to ensure even coating (approximately 30 ml of sigmacote® is retained prior to washing) and then the beads are washed with de-ionised water, prior to drying at 30 °C for 16 h. The surface energy of the beads is characterised by the drop test method [14], where the balance of cohesive force, given by JKR model [15] and detachment force for a critical particle size, which is identified by microscopy, enables the calculation of surface energy.

The 50 mm diameter FT4 vessel with the 48 mm impeller is used (Fig. 2). The standard test procedure is applied to the bed of glass beads, whereby the bed is initially conditioned by rotating the impeller clockwise to gently slice the bed surface and produce a reproducible, low stress packing state. The cell is then split to remove any material above a bed height of 80 mm. Following this step the test is carried out with a tip speed of 100 mm/s and a helix angle of 5° (full blade velocity details given in Table 1) by rotating the blade anti-clockwise, thus driving into the powder bed. The vertical force acting on the base, F_{base}, and the torque acting on the impeller, T, are measured at approximately 200 μm increments of vertical displacement. The flow energy,

$$E_{flow} = \int_0^H \left(\frac{T}{R \tan \alpha} + F_{base} \right) dH, \tag{1}$$

where R is the impeller radius, α is the helix angle and H is the penetration depth. The total flow energy corresponds to a penetration depth of 70 mm (10 mm from the base).

The FT4 operation described above is simulated by DEM using the EDEM code of DEM Solutions (Edinburgh, UK). Approximately 25,000 particles are generated in a column with a height of 0.5 m and allowed to descend under gravity to produce a bed height of 80–85 mm, after which particles above a height of 80 mm are removed. Since the initial packing fraction at the point of generation is low, the bed preparation procedure is not expected to influence the resulting flow energy, hence the conditioning step is ignored in the simulations. In order to accurately account for the cohesive nature of the beads, whilst ensuring adequate simulation times, the linear elastic plastic and adhesive model of Pasha et al. [16] is used (Fig. 3). The elastic and plastic stiffnesses, k_e and k_p, respectively, were measured by compressing 25 individual beads to a load of 1 N using an Instron Mechanical Testing machine (model 5566). The particle–particle and particle–wall friction coefficients are estimated to be 0.1 in the first instance; however the influence of particle–particle sliding friction on the resulting flow energy is investigated. The simulated material properties and interaction properties are given in Tables 2 and 3, respectively. The critical time-step, t_{crit}, is 1.15×10^{-5} s, consequently a time step of 2.29×10^{-6} s ($0.2\ t_{crit}$) is used.

3. Results and discussion

3.1. Experimental

The cohesivity of the silanised glass beads as used in the experiments was insufficient to be characterised by the drop test directly, instead

Table 1
FT4 impeller operational speeds.

Description	Start height (mm)	End height (mm)	Helix angle (°)	Tip speed (mm/s)	Vertical velocity (mm/s)	Rotational speed (rad/s)
Conditioning down	110	10	5	−60	−5.23	2.49
Global auto-turn	10	1	2	−60	−2.09	2.49
Conditioning up	1	100	−5	60	5.23	2.49
Test down	100	10	−5	100	−8.72	−4.15
Global auto-turn	10	1	2	−60	−2.09	2.49
Conditioning up	1	100	−5	60	5.23	2.49

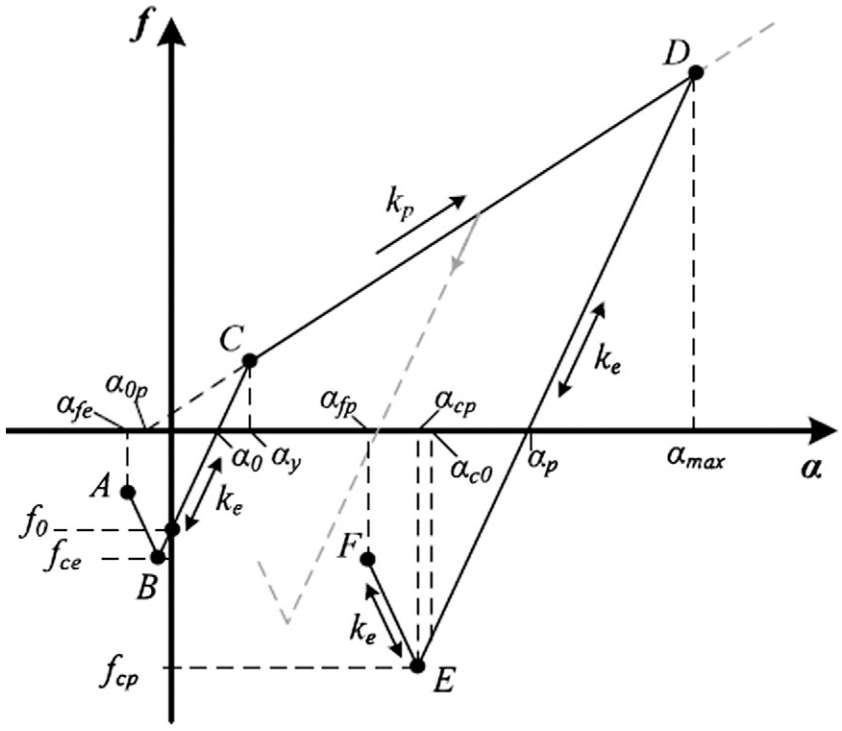

Fig. 3. Contact model of Pasha et al. [16].

smaller glass beads were also silanised following the same procedure and used in the drop test method to measure the surface energy. In the work of Zafar et al. [14], the drop velocity was varied resulting in particles of different sizes detaching from the substrate, yet giving similar surface energy values. This is therefore assumed to be the case here too, i.e. the surface energy being independent of particle size. Thus glass beads of 63–125 μm sieve sizes were coated with Sigmacote® supplied by Sigma-Aldrich®. The silanised beads were dispersed onto a silanised 7 mm diameter glass slide using the dispersion unit of the Malvern Morphologi G3®. The size distributions before and after the test were also measured with the Malvern G3. A drop height of 40 mm was used, which provided an impact velocity of 4 m/s, from which the surface energy was estimated using the approach of Zafar et al. [14]. The surface energy of these coated glass beads was estimated to be 29 mJ/m^2 and used in the elastic plastic and adhesive model of Pasha et al. [16] in the EDEM code.

The glass beads were poured into the FT4 vessel and tested under the operational conditions described in Section 2. Four separate powder beds were tested. The average flow energy for these tests is shown in Fig. 4 along with the error bars indicating the standard deviation, where good reproducibility is obtained.

3.2. DEM simulations

The flow energy in the DEM simulations was calculated from the torque on the blade and downward force on the base of the vessel using Eq. (1). The resulting flow energy values for the simulations and experiments of the silanised glass beads are shown in Fig. 5. The simulations underestimate the flow energy measured experimentally by about 28% at full penetration, with the total flow energy found to be 639 and 891 mJ in the simulations and experiments, respectively. This discrepancy may be due to the coefficient of sliding friction used being too low (0.1). To address this, the simulations were repeated using particle-particle sliding friction coefficients of 0.2, 0.3, 0.4 and 0.5. Fig. 6 shows the variation in total flow energy with sliding friction. There is a notable increase in flow energy as μ_s is increased, although this change is more substantial at lower friction values. Such behaviour is expected,

Table 2
Simulation material properties.

Material property	Particles	Geometries
Density (kg/m^3)	2450	7800
Elastic stiffness, k_e (kN/m)	37.8	74.9
Plastic stiffness, k_p (kN/m)	25.4	–
Plastic-adhesive stiffness, k_{cp} (N/m)	0.21	–

Table 3
Simulation interaction properties.

Material property	Particle–particle	Particle-geometry
Coefficient of restitution	0.4	0.4
Coefficient of sliding friction, μ_s	0.1 (0.1–0.5)	0.1
Coefficient of rolling friction, μ_r	0.01	0.01
Interface energy (mJ/m^2)	29	0

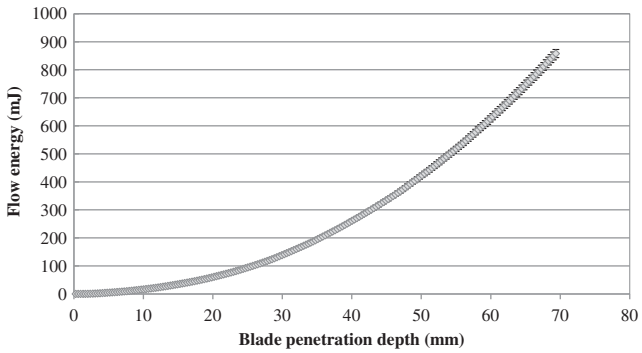

Fig. 4. The flow energy of the coated glass beads.

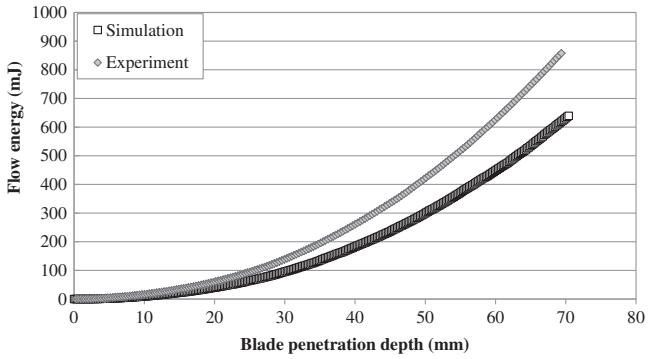

Fig. 5. Comparison of the experimental and simulated glass beads coated with hexane functional group.

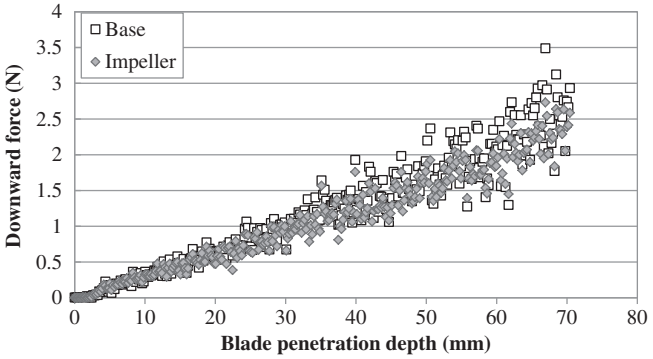

Fig. 7. The vertical forces acting on the base and the blade.

as shown by Gröger and Katterfeld [17] who found that increasing μ_s beyond 0.5 had limited effect on the angle of internal friction.

The flow energy accounts for the resistance to movement of the blade, hence it would be expected that the downward force contribution used in the calculation should be that acting on the blade. However, the experimental device uses the downward force acting on the base to determine the vertical work. The DEM allows the forces acting on all particles and walls to be estimated, which means the vertical force acting on the base and the blade can be compared. This is shown in Fig. 7, where the force acting on the base is very similar to that acting on the impeller, but is marginally greater throughout the entirety of the test. The flow energy was also calculated using Eq. (1) with the force acting on the impeller, this is compared to the flow energy using the force acting on the base in Fig. 8. The flow energies using the force acting on the impeller and on the base are 632 and 639 mJ, respectively. Therefore the slight discrepancy between the force on the base and the impeller has a negligible contribution to the flow energy, thus suggesting that the resistance to flow is predominantly rotational, i.e. $T/R\tan\alpha \gg F_{base}$. Further investigations into operation under different helix angles or blade geometries may shed light as to why this is the case.

The DEM simulations allow the internal bed stresses and velocities to be assessed. Here we consider the stresses immediately in front of the blade, within three measurement regions that span the width of the blade, as shown in Fig. 9. The measurement cells are 10 mm high (equal to the blade), 6.3 mm wide and 6 mm deep, and are in direct contact and aligned with the leading face of the impeller. The normal and shear stresses within the measurement cells are estimated by considering the forces acting on all particles in the cell using Eq. (2),

$$\sigma_{ij} = \frac{1}{V}\sum_{1}^{N} F_{ij} \cdot r, \tag{2}$$

where V is the cell volume, N is the number of particles in the cell, and F is the force acting in direction i on face j of the particle [18], using Cartesian coordinates. From these stresses the major, intermediate and minor principal stresses are then calculated from the nine stress tensors by determination of eigenvalues. The deviatoric stress, τ_D, and average compressive stress, σ_H, are given by Eqs. (3) and (4), respectively [19].

$$\tau_D = \frac{\sqrt{(\sigma_1-\sigma_2)^2 + (\sigma_1-\sigma_3)^2 + (\sigma_2-\sigma_3)^2}}{\sqrt{6}}, \tag{3}$$

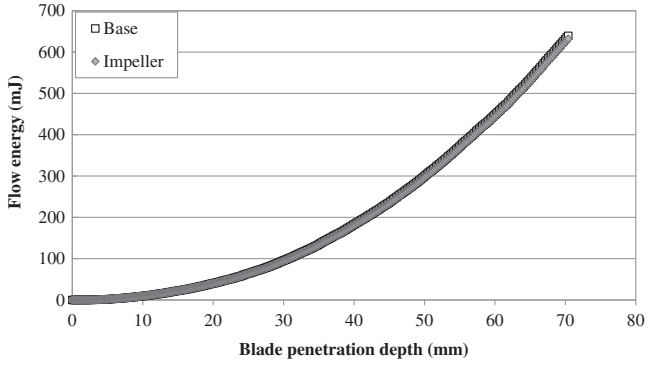

Fig. 8. The flow energy calculated using the vertical forces acting on the base and the impeller.

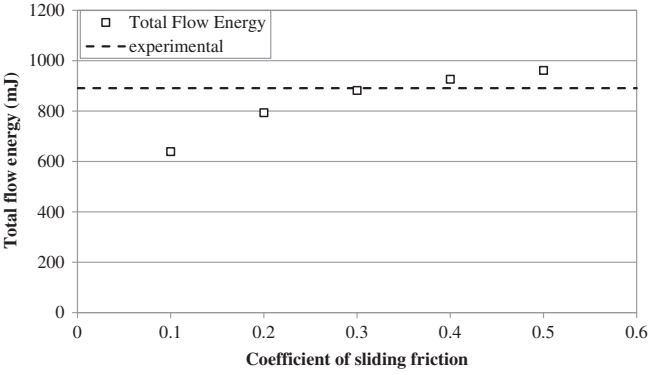

Fig. 6. Influence of sliding friction coefficient on total flow energy.

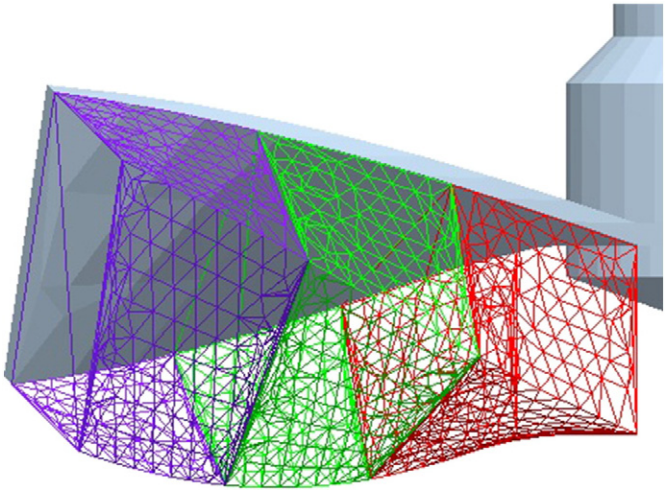

Fig. 9. Stress measurement cells used in the DEM.

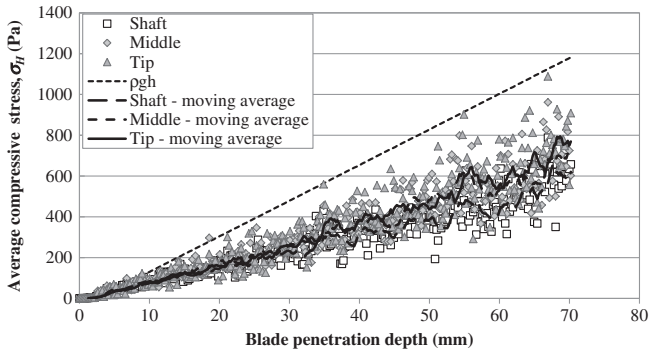

Fig. 10. Average compressive stresses during the simulated FT4 test.

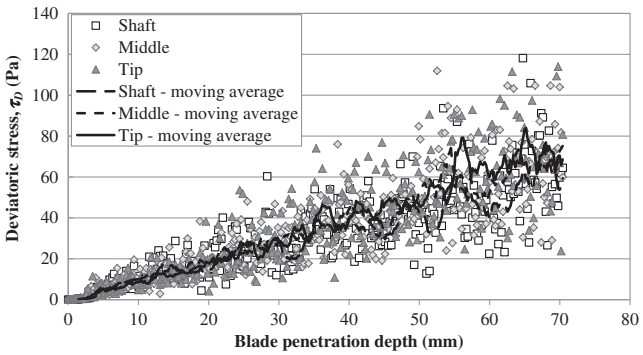

Fig. 11. Deviatoric stresses during the simulated FT4 test.

$$\sigma_H = \frac{\sigma_1 + \sigma_2 + \sigma_3}{3}, \tag{4}$$

The evolution of the average compressive stress in the three measurement cells is shown in Fig. 10, along with the hydrostatic head of the particles (ρgh), where ρ is the bulk density of the bed. The moving averages of 10 data points are shown by the dashed lines for the average compressive stress in each measurement cell. It can be seen that the average compressive stress continually increases as the blade descends further into the bed. The increase is approximately linear, as indicated by the moving averages. The increase is less than that of the hydrostatic stress, as would be expected since a portion of the stress is transferred laterally to the walls by friction. There is notable scatter in the data, which could be caused by the relatively small number of particles in each measurement cell (approximately 35–55 particles). Despite this scatter, it is clear that the average compressive stress values are strikingly similar in the three measurement cells, with a very slight increase in stress from the shaft towards the tip of the blade. This increase suggests that the bed is more mobilised by the impeller near the wall region.

The deviatoric stresses in the three measurement cells throughout the FT4 test are shown in Fig. 11, along with the corresponding moving averages of 10 data points. The scatter in the deviatoric stresses is more significant than the compressive stresses, however the moving averages clearly show an approximately linear increase in stress with blade penetration depth. The similarity in the deviatoric stresses across the length of the blade (radial direction) is remarkable, and suggests that the designed twist in the blade does indeed provide a roughly constant shear stress profile along the radial direction across the blade length.

4. Conclusions

The standard downward test procedure of the FT4 Powder Rheometer was carried out experimentally and also computationally simulated by the DEM. The simulations using a linear elasto-plastic and adhesive contact model underestimated the flow energy measured in FT4 experiments by about 28% at the maximum penetration depth. This is expected to be due to the value of sliding friction coefficient used in the simulations being too low. An increase in sliding friction coefficient from 0.1 to 0.5 caused an increase in the flow energy. The simulations show that the vertical force acting on the base is slightly greater than that acting on the impeller, however the flow energy is almost identical regardless of which force is used as the torque dominates the value of flow energy. The deviatoric and hydrostatic stresses in front of the blade were estimated from the DEM. The results suggest that the design of the FT4 blade provides a roughly constant shear stress along the blade length, i.e. in the radial direction. Further work will address the shear strain rate sensitivity, the influence of particle properties (such as shape and cohesion) on the shear flow behaviour and the relationship between the flow energy and powder yield stresses, as measured by the shear cell method.

Acknowledgments

The financial support of the Engineering and Physical Sciences Research Council, UK, through the Grant EP/G013047 is gratefully acknowledged.

References

[1] A.W. Jenike, Powder Technol. 1 (1967) 237–244.
[2] D. Schulze, A. Wittmaier, Flow properties of highly dispersed powders at very small consolidation stresses, Chem. Eng. Technol. 26 (2) (2003) 133–137.
[3] A. Castellanos, J.M. Valverde, M.A.S. Quintanilla, The Sevilla powder tester: a tool for characterizing the physical properties of fine cohesive powders at very small consolidations, KONA 22 (2004) 66–81.
[4] B. Formisani, P. Bernado, R. Girionte, A. Minnicelli, The bed support experiment in the analysis of the fluidization properties of fine solids, Proceedings of the Conference 4th World Congress on Particle Technology. Sydney (Australia) 2002, p. 373.
[5] K. Johanson, 2014. Personal Communication. Material Flow Equipment, LLC, 7010 NW 23rd Way, Suite A, Gainesville, FL 32653 USA, http://www.matflowsol.com.
[6] A. Hassanpour, M. Ghadiri, Characterisation of flowability of loosely compacted cohesive powders by indentation, Part. Part. Syst. Charact. 24 (2) (2007) 117–123.
[7] G.I. Tardos, S. McNamara, I. Talu, Slow and intermediate flow of a frictional bulk powder in the Couette geometry, Powder Technol. 131 (2003) 23–39.
[8] V.S. Kumar, T. Murthy, P.R. Nott, Rheometry of dense granular materials: the crucial effects of gravity and confining walls, Powder & Grains 2013 Proceedings 2013, pp. 49–51.
[9] M. Pasha, C. Hare, A. Hassanpour, M. Ghadiri, Numerical analyses of strain rate sensitivity in ball indentation on cohesive powder beds, Chem. Eng. Sci. 123 (2015) 92–98.
[10] R. Freeman, Measuring the flow properties of consolidated, conditioned and aerated powders — a comparative study using a powder rheometer and a rotational shear cell, Powder Technol. 174 (2006) 25–33.
[11] M. Leturia, M. Benali, S. Lagarde, I. Ronga, K. Saleh, Characterization of flow properties of cohesive powders: a comparative study of traditional and new testing methods, Powder Technol. 253 (2014) 406–423.
[12] R. Bharadwaj, W. Ketterhagen, B. Hancock, Discrete element simulation study of a Freeman powder rheometer, Chem. Eng. Sci. 65 (2010) 5747–5756.
[13] C. Hare, M. Ghadiri, R. Dennehy, Prediction of attrition in agitated particle beds, Chem. Eng. Sci. 20 (2011) 4757–4770.
[14] U. Zafar, C. Hare, A. Hassanpour, M. Ghadiri, Drop test: a new method to measure the particle adhesion force, Powder Technol. 264 (2014) 236–241.
[15] K. Johnson, A. Kendall, Surface energy and the contact of elastic solids, Proc. R. Soc. Lond. A Math. Phys. Sci. 324 (1971) 301–313.
[16] M. Pasha, S. Dogbe, C. Hare, A. Hassanpour, M. Ghadiri, A new linear contact model for elasto-plastic and adhesive contacts in distinct element method, Granul. Matter 16 (2014) 151–162.
[17] T. Gröger, A. Katterfeld, On the numerical calibration of discrete element models for the simulation of bulk solids, 16th European Symposium on Computer Aided Process Engineering 2006, pp. 533–538.
[18] K. Bagi, Stress and strain in granular assemblies, Mech. Mater. 22 (1996) 165–177.
[19] S. Luding, Constitutive relations for the shear band evolution in granular matter under large strain, Particuology 6 (2008) 501–505.